Effects of Structural Change Induced by Physical Aging on the Biodegradation Behavior of PLGA Films at Physiological Temperature

Taiyo Yoshioka, Naoki Kawazoe, Tetsuya Tateishi, Guoping Chen*

The effects of structural changes induced by physical aging (namely, enthalpy relaxation) on the biodegradability of PLGA films at physiological temperature (37 °C) is investigated. The degradation rate and behavior of aged and non-aged PLGA films are compared, and the effects of physical aging on the biodegradability of the PLGA film are determined. Prior to the degradation experiments, aged films are prepared by annealing the amorphous PLGA films at 25 °C for 5 d or more. The degradation rate of aged films in accelerated degradation tests using aqueous NaOH is higher than those of non-aged films due to heterogeneous microscopic structural changes that occur during the aging process.

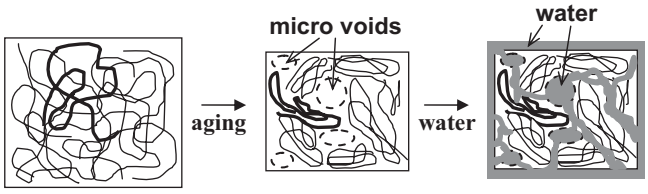

Introduction

When flexible polymers are in a molten state (shown as state A in Figure 1), the molecular chains are entangled with each other, forming random coils, and each polymer chain is in high energy state.[1] If melted polymer chains are quenched at a temperature that is sufficiently lower than the glass transition temperature (T_g), the chains freeze (Figure 2a) in a high energy, random coil state, which drastically reduces their segmental mobility, and results in an amorphous glass. However, by slowly annealing the material at a temperature (T_a) close to but below T_g, amorphous glass can undergo energetic relaxations (also called structural relaxations) from the non-equilibrium structural state to a more energetically stable state (from state C to D or E in Figure 1). Energetic relaxation, also known as enthalpy relaxation or physical aging, alters the structural, physical, and mechanical properties of the material. For instance, aging can increase the density and decrease the specific volume, enthalpy, and fracture strain of a polymer.[1b,c] The formation of amorphous glass can be achieved not only via quenching of melt but also via rapid evaporation of the solvent from solution.[2] Despite numerous studies on the physical aging of various polymers, the mechanism of structural changes at the molecular level remains unclear.

The degradation of biodegradable polyesters in vivo commonly proceeds through hydrolysis of the ester bonds in the polymer backbone, and the degradability of polyesters is strongly dependent on factors that affect the diffusibility of water molecules, such as the hydrophilicity, molecular weight, crystallinity and bulk shape of the polymer.[3] In addition, structural changes caused by physical aging is considered to affect the diffusibility of water and the biodegradability of polymers. Two possible diametrical effects of structural changes on the degradation behavior of polyesters were assumed. Specifically, if the degradation rate decreased upon physical aging, structural changes could be explained by simple volume contraction, as shown in Figure 2b. Alternatively, if the degradation rate increased, microscopic, heterogeneous, structural fluctua-

T. Yoshioka, N. Kawazoe, T. Tateishi, G. Chen
Biomaterials Center, National Institute for Materials Science, 1-1 Namiki, Tsukuba, Ibaraki 305-0044, Japan
E-mail: guoping.chen@nims.go.jp

DOI: 10.1002/mame.201100109

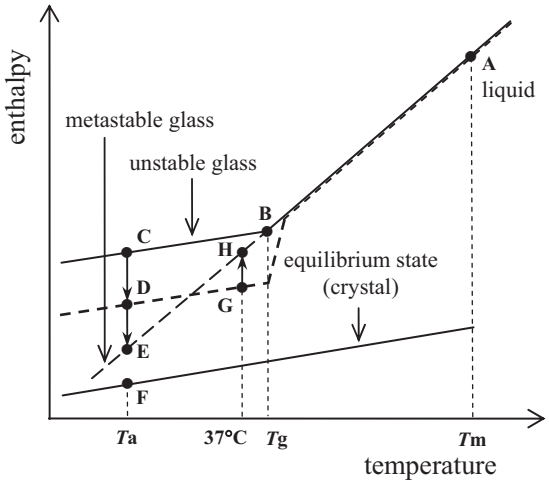

Figure 1. Enthalpy/temperature diagram. T_m is the melting temperature, T_g is the glass transition temperature, and T_a is the annealing temperature. In this report, the enthalpic change from C to D or C to E is referred to as the enthalpy relaxation or physical aging, and the change from G to H is referred to as enthalpy recovery.

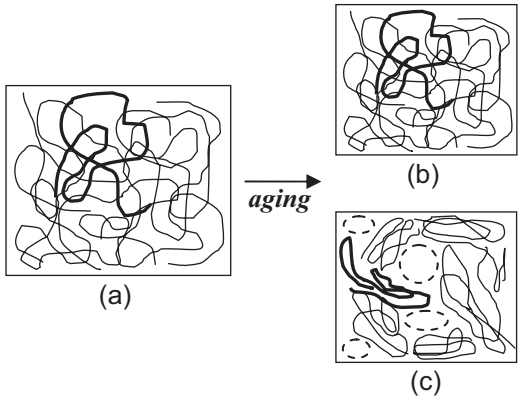

Figure 2. Schematic models of the two-diametrical structural changes accompanied by enthalpy relaxation [(a) to (b) and (a) to (c)]. The model (a) indicates that a random coil structure is prevalent in the quenched amorphous glass. During physical aging, the amorphous glass undergoes a macroscopic volume contraction keeping with the random coil structure (b) and accompanying with a microscopic heterogeneous fluctuations (c). In each model, identical molecular chains are depicted with a thick line. Areas enclosed with a broken line represent micro voids formed during the aging process.

tions in the local chain packing occurred during macroscopic volume contraction, leading to an increase in the water permeability of the film, as shown in Figure 2c. In this study, only α-relaxation,[4] which is responsible for T_g and can be detected through differential scanning calorimetry (DSC) techniques, was considered. β-relaxation,[4] which is associated with local intramolecular motion, was not considered because the effects of β-relaxation on the degradation behavior of the polymer are negligible compared to the effects of α-relaxation.

Studies on the physical aging of biodegradable polyesters have been limited. However, due to the recent evolution of medical fields that depend on the performance of biodegradable polymers, such as controlled drug delivery systems and tissue engineering, the number of studies on the physical aging of biodegradable polymers has increased.[2,5] Poly[(lactic acid)-*co*-(glycolic acid)] (PLGA) behaves as an amorphous polymer over a wide range of copolymer composition ratios (from 25/75 to 75/25), and the T_g of PLGA is approximately 35–55 °C.[3b,c] Thus, ambient and physiological conditions for the manufacturing, storage and use of PLGA induce serious physical aging. Allison et al.[2] found that structural relaxation in amorphous PLGA microparticles in drug delivery systems can decrease burst release of drug molecules due to an increase in particle density and a decrease in porosity. However, a systematic study of the effects of physical aging on the biodegradability of biodegradable polyesters has not yet been reported due to variety of experimental difficulties. As described in our recent study on the in vitro degradation of PLGA sponges, the main difficulty associated with biodegradable polyesters, which has its T_g at around physiological temperature, is that physical aging and degradation occur simultaneously in physiological environments.[6] To successfully evaluate the effects of physical aging on polymer biodegradability, physical aging and degradation behavior must be investigated individually. In this study, the effects of the aging conditions on enthalpy relaxation and the mechanical properties of PGLA, which are one of the most practically used biomaterials and whose T_g is near but above the physiological temperature, were investigated through DSC and tensile tests, respectively. Before the degradation test, an optimum experimental condition, in which both relaxation and recovery of enthalpy did not occur significantly during the degradation test, was explored. Then, the kinetic parameters of the physical aging process of PLGA were evaluated at 25 °C. Finally, the degradation behavior of aged and non-aged PLGA films was compared.

Experimental Section

Materials

PLGA pellets with a copolymer ratio of 75/25 (D,L-lactic acid/glycolic acid) were purchased from Sigma-Aldrich, Inc. (St. Louis, MO). The weight-average ($\overline{M}_w$) and number-average ($\overline{M}_n$) molecular weights, and the polydispersity index (PDI) of the PLGA pellets were measured by gel permeation chromatography (GPC), and values of 109 520 ± 1 670, 47 870 ± 1 560, and 2.3 ± 0.1 were obtained, respectively.

Gel Permeation Chromatography (GPC)

$\overline{M}_w$, $\overline{M}_n$, and PDI of the PLGA pellets were determined by GPC on a high-performance liquid chromatography system (HLC-8220GPC, Tosoh Co., Tokyo, Japan) equipped with two TSK gel columns (GMH_{HR}-M, Tosoh Co., Tokyo, Japan). Chloroform at a flow rate of 1.0 mL · min^{-1} at 40 °C was used as the elution solvent. TSK polystyrene standards (Tosoh Co., Tokyo, Japan) were used to calibrate the system.

Differential Scanning Calorimetry (DSC)

The enthalpy relaxation of aged films was determined via DSC instrument, DSC8240 (Rigaku Co., Tokyo, Japan). In addition, to induce physical aging, some of the annealing treatments were performed by DSC. All of the DSC measurements and annealing treatments were conducted on 5.00 ± 0.05 mg of sample under a flow of nitrogen gas at a rate of 50 mL · min^{-1}. In general, each DSC measurement consisted of the following steps: (1) heating from −20 to +200 °C; (2) cooling from +200 to −20 °C; (3) heating from −20 to +200 °C. All steps were conducted at a scan rate of 10 °C min^{-1}. Only the DSC curves obtained from heating steps 1 and 3 were recorded and were labeled as the 1st and 2nd scan, respectively. The instrument was calibrated with indium, tin, and lead. Heating rates, cooling rates, and individual programs were altered depending on the purpose of the experiment. The enthalpy of relaxation (ΔH) was estimated by integrating the endothermic peak of enthalpy recovery at the glass transition (see image in the section 'The Effects of the Annealing Temperature on the Enthalpy of Relaxation', below).

Preparation of PLGA Amorphous Films and the Annealing Treatment Used to Induce Physical Aging

Determination of the Melting Conditions for the Preparation of Pure Amorphous Films

PLGA cast film was fabricated by casting a 10 wt% PLGA solution in chloroform on a Teflon mould plate with a diameter of 40 mm and a depth of 1.6 mm at room temperature. The cast solution was degassed to remove air bubbles, air-dried for 2 d without accurate control of the evaporation rate, and vacuum-dried for another 3 d.

Figure 3 shows a typical DSC curve for the cast film, measured at a scanning rate of 10 °C · min^{-1} from −15 to +200 °C. During the 1st scan, a distinct endothermic peak attributed to the melting of crystals was obtained. The reproducibility of the melting temperature (T_m) was poor due to uncontrolled crystallization or due to inhomogeneous composition of the copolymer; however, the T_m generally appeared between 140 and 180 °C, and was always less than 200 °C. Thus, pure amorphous films were prepared via DSC at 200 °C for 10 min. The complete removal of the crystalline history under these melting conditions was confirmed by a complete disappearance of the endothermic peak during the 2nd scan, as shown in Figure 3.

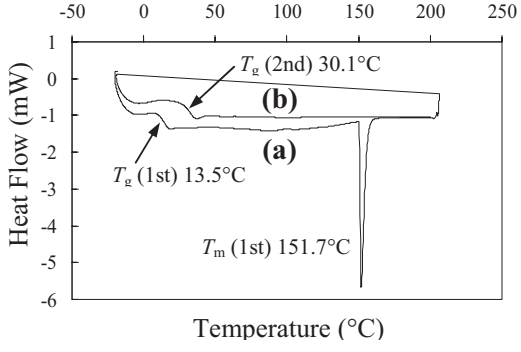

Figure 3. DSC curves of the cast film: (a) 1st scan and (b) 2nd scan.

Preparation of Amorphous Films

According to the procedure outlined in last section, the PLGA film was sandwiched between smooth aluminium plates, hot-pressed at 200 °C for 10 min, and quenched with liquid nitrogen. The thickness of the resultant amorphous film was approximately 0.2 mm.

Annealing Treatment Used to Induce Physical Aging

In the relaxation experiments, the amorphous film was immediately annealed under predetermined annealing conditions. For an annealing time (t_a) of 2 h or less, annealing treatments were conducted via DSC under a flow of nitrogen gas, and the enthalpy of relaxation was measured immediately. Alternatively, for a t_a greater than 2 h, the annealing treatments were conducted in a thermostated hotplate (Thermo Plate TP-80, AS-ONE Co., Osaka, Japan), and the enthalpy of relaxation of the annealed sample was immediately evaluated via DSC. The quenched amorphous film was weighed, sealed in an aluminium pan, and placed into the DSC instrument. To suppress the undesirable effects of ambient temperature, samples with a t_a of 2 h or less were prepared within 10 min. In addition, films that were annealed on the thermostated hotplate were immediately weighed, sealed into an aluminium pan, and placed into the DSC instrument within 10 min, and DSC measurements were conducted immediately.

To compare the physical properties of aged and non-aged films, the quenched amorphous film was immediately cut into two pieces to produce a pair of films with an identical thickness and thermal history. One of the films was annealed, and the other was stored in the freezer (−20 °C) to preserve its amorphous structure during the annealing treatment of the tally. The detailed process for the determination of optimal annealing condition is described in the Results and Discussion.

Tensile Tests

The tensile properties of aged and non-aged films (20 × 5 × ≈0.2 mm^3) were measured at room temperature with a Texture Analyzer TA-XT Plus (Stable Micro Systems Ltd., Surrey, UK) at a cross-head speed of 2 mm · min^{-1}. The thickness of each film was measured using micrometer, and the reported tensile properties are the average obtained from seven specimens. The tensile modulus was estimated from the tangent of the initial slope of the stress/strain curve.

Degradation Tests

The degradation behavior of aged and non-aged films (7 × 7 × ≈0.2 mm^3) was determined in 0.1 M aqueous sodium

hydroxide (NaOH aq) at 37 °C under constant agitation (60 shakes per min). In each experiment, the ratio of the volume of NaOH aq to the mass of film was greater than 100. After the degradation tests were complete, the films were collected, washed with deionized water, air-dried for 1 d, and vacuum-dried for 3 d. The weight (W_t) of dried and degraded films was measured with an electrical balance (AG 135, Mettler-Toledo International Inc., NY, USA), and the weight loss was calculated according to a simple equation:

$$\text{Weight loss}(\%) = \frac{(W_0 - W_t)}{W_0} 100 \quad (1)$$

where W_0 is the initial weight of the sample.

Results and Discussion

Determination of the Optimal Conditions of the Annealing Treatment and Degradation Tests

To evaluate the effects of physical aging on the biodegradability of biodegradable polyesters, relaxation and recovery of enthalpy must be avoided during the degradation tests. On the other hand, shorter annealing times are preferable due to practical reasons. Thus, the optimal conditions for the annealing treatments and degradation tests were explored by conducting the following three steps.

The Effects of the Annealing Temperature on the Enthalpy of Relaxation

The 2nd scan of DSC was performed on five samples of aged films, and the average T_g was 41 ± 0.9 °C. The Vogel-Tamman-Fulcher (VTF) equation (Equation 2),[7] which relates the relaxation time (τ) to T_a, suggests that an increase in T_a (namely, the closer to the T_g), results in an decrease in τ. In the VTF equation, τ_0 is a relaxation constant, D is Angell's strength,[5c] and T_0 is the zero mobility temperature, also known as the Vogel temperature. Typically, the Vogel temperature of a polyester film is ≈50 °C less than T_g.[5b]

$$\tau = \tau_0 \exp\left(\frac{DT_0}{T_a - T_0}\right) \quad (2)$$

In contrast, the enthalpy of relaxation is restricted by the energy of metastable glass; therefore, a potential relaxation decreases as the T_a approaches the T_g (see Figure 1). To determine the appropriate T_a of a temporal annealing time of 4 d, the following annealing temperatures were evaluated: (a) 40, (b) 30, (c) 25, and (d) 15 °C. The 1st scan DSC curves obtained from PLGA films aged at different T_as are shown in Figure 4. The results indicated that the area of the endothermic peak (ΔH) was highly dependent on the T_a. For instance, the highest ΔH was obtained at a T_a of 25 °C, followed by 15, 30, and 40 °C. These results do not agree with

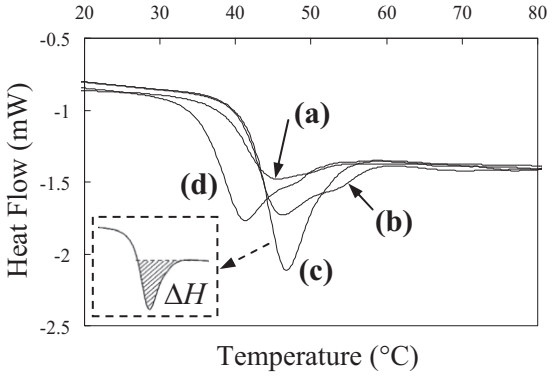

Figure 4. DSC curves of aged films annealed at (a) 40, (b) 30, (c) 25, and (d) 15 °C for 5 760 min (4 d). All of the curves were obtained from the 1st scan. Inset shows an example showing how the ΔH was estimated from the curve (c).

those predicted by the VTF equation (Equation 1), which suggests that ΔH should increase with an increase in T_a. This disparity was attributed to the achievement of the potential relaxation at a T_a of 40 and 30 °C, during the annealing time. Based on these results, the optimal T_a was 25 °C.

Effect of Annealing Time on the Enthalpy of Relaxation

To determine the optimal t_a at $T_a = 25$ °C, the relationship between the t_a and the ΔH of samples annealed at 25 °C was determined. A plot of ΔH at 25 °C as a function of the t_a (from 0 to 360 h) is shown in Figure 5. The results indicated that ΔH increased with an increase in the t_a. The dependence of ΔH on the t_a can be explained by the Cowie-Ferguson equation (Equation 3), which is based on the Kohlrausch-

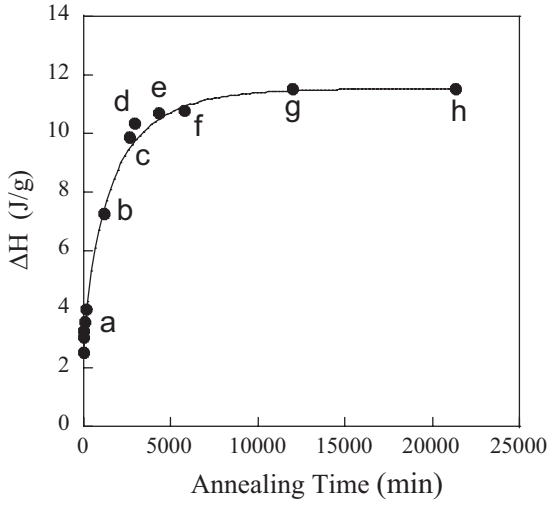

Figure 5. Enthalpy relaxation at 25 °C as a function of the annealing time: (a) 0–120, (b) 1 200 (20 h), (c) 2 640 (44 h), (d) 2 880 (48 h), (e) 4 320 (72 h), (f) 5 760 (96 h), (g) 12 000 (200 h), and (h) 21 600 min (360 h). The solid line represents the fit of the Cowie-Ferguson model.

Williams-Watts stretched exponential function. In the Cowie-Ferguson equation, ΔH_∞ is the enthalpy as t_a approaches ∞ (namely, the enthalpy difference between the glassy and metastable state of the polymer) and β is a non-exponential fitting parameter that reflects the distribution of relaxation times among molecules ($0 < \beta \leq 1$, and $\beta = 1$ implies a single relaxation mode).[8]

$$\Delta H(t_a) = \Delta H_\infty \left[1 - \exp\left\{-\left(\frac{t_a}{\tau}\right)^\beta\right\}\right] \quad (3)$$

As shown in Figure 5, the Cowie-Ferguson model best fit the experimental data at a ΔH_∞, τ, and β of 11.54 J · g^{-1}, 1 600 min, and 0.77, respectively. Moreover, the results indicated that enthalpy relaxation was significant in the first 2 d of the aging process; however, relaxation decreased dramatically after the first 2 d and remained constant after 5 or 6 d.

To evaluate the effect of the annealing time on physical aging, the relationship between the annealing time and the mechanical properties of the films was also investigated. Typical stress/strain curves of the non-aged film (a) and the film aged at 25 °C for 7 d (b) are shown in Figure 6. The fracture strain of the aged film was dramatically lower than that of the non-aged film; however, the tensile modulus and yield strength of both films were almost identical. A decrease in the fracture strain (or embrittlement) is commonly observed as a result of physical aging in various kinds of amorphous polymers.[9] Moreover, in poly(L-lactic acid) (PLLA), a representative biodegradable polyester, significant embrittlement due to physical aging at physiological temperature was reported by Celli and Scandola[10] and Pan et al.[11] Although Celli and Scandola ascribed the observed embrittlement to a decrease in the ability to dissipate energy through molecular motion, Pan et al. attributed the embrittlement to a change in the conformation of the molecular chains from disordered to locally ordered, which is similar to the concept of molecular

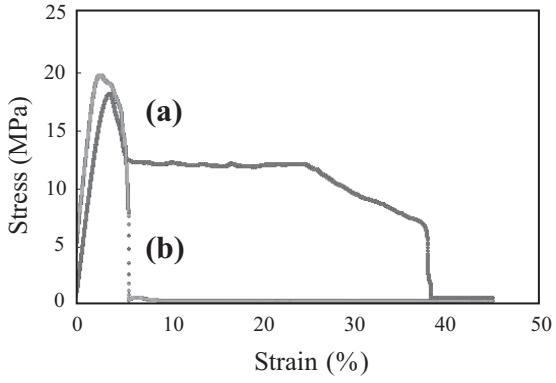

Figure 6. Typical stress/strain curves of the films: (a) before and (b) after aging at 25 °C for 10 080 min (7 d).

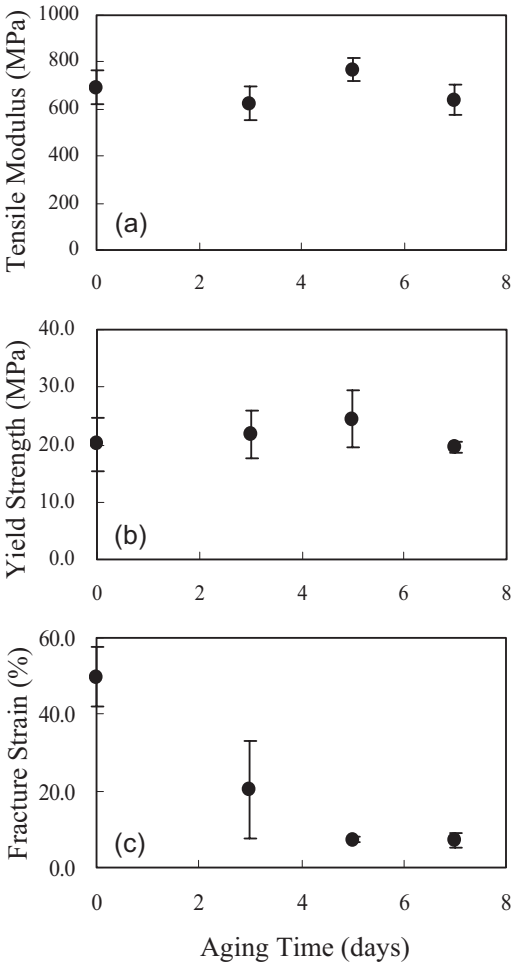

Figure 7. (a) Tensile modulus, (b) yield strength, and (c) fracture strain of non-aged films and films aged at 25 °C as a function of aging time (d). Data represent the average ± SD of seven samples.

rearrangement shown in Figure 2c. The tensile modulus, yield strength, and fracture strain of non-aged films and films aged at 25 °C for 3, 5, and 7 d are shown in Figure 7. Although the tensile modulus and yield strength of the films did not change significantly throughout the entire aging period, the fracture strain decreased dramatically from 49.8 ± 7.8 to 20.1 ± 12.7% in the first 3 d and to 7.3 ± 0.7% in the first 5 d. However, at an aging time greater than 5 d, the fracture strain of aged films remained constant. These results indicated that structural changes due to physical aging were complete within 5 d, which agrees with the results shown in Figure 5. Thus, in the preparation of aged films for subsequent degradation tests, the t_a was set to 5 d.

Effect of Degradation Test Temperature on Enthalpy Recovery

As previously mentioned, to evaluate the effects of physical aging on the biodegradability of a polymer, further

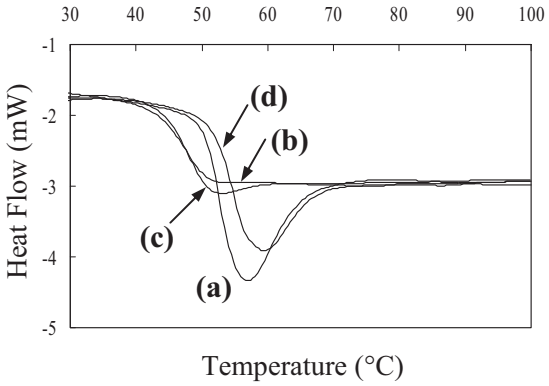

Figure 8. DSC curves of aged film annealed at 25 °C for 10 080 min (7 d): (a) control, (b)–(d) reannealed films. Reannealing conditions: (b) 39 °C for 1 440 min (24 h), (c) 37 °C for 2 880 min (48 h), and (d) 37 °C for 1 440 min (24 h). All of the curves were obtained from the 1st DSC scan.

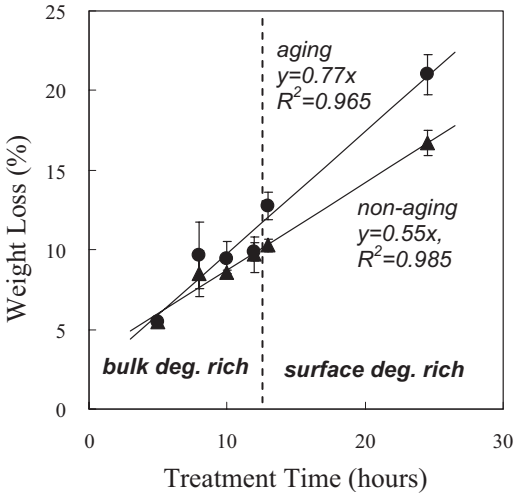

Figure 9. The relationships between the weight loss and treatment time of aged (●) and non-aged (▲) films. Hydrolytic treatments were conducted with 0.1 M NaOH at 37 °C. Data represent the average ± SD of four samples.

enthalpy relaxation and enthalpy recovery, which is represented by a state change from G to H in Figure 1, should be avoided during degradation tests at physiological temperature (37 °C). The time dependence of the enthalpy change of aged films at 37 and 39 °C (for comparison) was investigated by DSC (see Figure 8). As shown in the figure, thermal treatment at 37 and 39 °C is labeled as reannealing to distinguish it from the first annealing process used to induce physical aging. The results indicated that almost complete enthalpy recovery occurred during reannealing at 39 °C for 24 h and at 37 °C for 48 h [see (b) and (c) in Figure 8, respectively]. However, compared to non-reannealed sample (Figure 8a), only 13% enthalpy was recovered when aged samples were reannealed at 37 °C for 24 h (Figure 8d); thus, the specimen remained in a high energy state ($\Delta H = 10.01\ J \cdot g^{-1}$) corresponding to that of plot d (aged at 25 °C for 48 h) in Figure 5. Therefore, the maximum reannealing time (namely, the time of the degradation test) at 37 °C was determined to be 24 h.

Degradation Test

Due to the aforementioned time constraints (<24 h), NaOH was used to achieve accelerated degradation at 37 °C. In a preliminary test, the appropriate concentration of aqueous NaOH was determined to be 0.1 M (the degradation rates corresponding to 0.5 and 0.05 M were too fast and too slow, respectively). Figure 9 shows the relationship between weight loss and alkaline treatment time of aged and non-aged films. The results indicated that the degradation rates of aged films were faster than those of non-aged films, indicating that structural changes caused by physical aging are not due to homogeneous volume contraction, as depicted in Figure 2b. Furthermore, the results implied that volume contraction with concomitant microscopic heterogeneous structural fluctuations occurred during the aging process, leading to accelerated water diffusion, as depicted in Figure 2c. Several authors also propose the formation of density fluctuations or locally ordered domains during physical aging.[12] A recent report on PLLA by Pan et al.[13] suggested that the induction period for crystallization decreases as physical aging proceeds, and the cold-crystallization rate is enhanced by the aging process due to conformational and microstructural chain-rearrangements that occur during the aging process, which can act as nucleation precursors in subsequent crystallizations. In this study, the rapid degradation of aged films can be explained by a similar structural change.

Hydrolytic degradation of non-crystalline biodegradable polyesters can occur via surface or bulk degradation. Surface degradation occurs only on the bulk surface of the polymer, and bulk degradation proceeds uniformly and perpendicularly to the surface of the polymer.[6a,14] Surface and bulk degradation are related to weight loss and the loss of molecular weight, respectively.[6a,14] In bulk degradation, acidic degradation products, which act as a catalyst in successive hydrolytic reactions, may accumulate inside of the polymer matrix due to the low diffusion rate. As a result, the polymer core displays a faster degradation rate than outer regions of the polymer. This type of degradation is referred to as autocatalyzed bulk degradation.[6a,15] In Figure 9, the difference of degradation rate between aged and non-aged films at early stage is not so clear; however, becomes more apparent at the later stage (after approximately 13 h). This can be attributed to more preferential autocatalyzed bulk degradation in aged films than in non-aged films at early stage, providing further evidence for microscopic structural fluctuations in the aged films. In the

aged films, structural fluctuations that arise during the aging process result in low density regions, where penetration and successive diffusion of water molecules is easier than in higher density areas of aged films or the homogeneous structure of non-aged films. As a result, autocatalyzed bulk degradation is more preferential in aged films than in non-aged films at early stages of the degradation process (first 13 h). However, the degree of autocatalyzed bulk degradation in the early stages of the process does not significantly affect weight loss. On the other hand, due to the high degree of autocatalyzed bulk degradation in the early stage of the degradation process, the surface area of aged films increases dramatically. Then, after 13 h, the dominant mechanism of degradation changes to surface degradation.[6a] As a result, subsequent surface degradation in aged films leads to substantial weight loss which is much lager than the one of non-aged films.

Conclusion

The effect of structural changes induced by physical aging on the degradability of PLGA films, with a T_g of 41 ± 0.9 °C, at physiological temperature (37 °C) was investigated. Before the degradation test, an optimum test condition, in which both relaxation and recovery of enthalpy did not occur significantly during the degradation test, was designed. As a result, only the effects of physical aging prior to the degradation tests were evaluated. The results, that the degradation rate of aged films was faster than that of non-aged films, indicated that a homogeneous structural contraction did not occur upon physical aging. Alternatively, a heterogeneous structural contraction accompanying microscopic structural fluctuations resulted in structural changes during the aging process. Furthermore, the degradation rate of aged films at early stages of the degradation process was similar to that of non-aged films; however, the degradation rate of aged films became faster at later stages, suggesting that the dominant mechanism of aged film degradation changed from autocatalyzed bulk degradation to surface degradation.

Received: March 23, 2011; Published online: July 5, 2011; DOI: 10.1002/mame.201100109

Keywords: annealing; biodegradable polyesters; degradation; physical aging; PLGA films

[1] [1a] J. M. Hutchinson, *Prog. Polym. Sci.* **1995**, *20*, 703; [1b] U. W. Gedde, *Polymer Physics*, Kluwer Academic Publisher, Dordrecht **1995**; [1c] I. M. Hodge, *Science* **1995**, *267*, 1945.
[2] S. D. Allison, *J. Pharm. Sci.* **2008**, *97*, 2022.
[3] [3a] W. Amass, A. Amass, B. Tighe, *Polym. Int.* **1998**, *47*, 89; [3b] Y. Ikada, "Tissue Engineering: Fundamentals and Applications" in: *Interface Science and Technology*, Vol. 8, Academic Press/Elsevier, New York **2006**; [3c] L. S. Nair, C. T. Laurencin, *Prog. Polym. Sci.* **2007**, *32*, 762; [3d] N. Lucas, C. Bienaime, C. Belloy, M. Queneudec, F. Silvestre, J. E. Nava-Saucedo, *Chemosphere*, **2008**, *73*, 429.
[4] [4a] S. Vyazovkin, I. Dranca, *Pharm. Res.* **2006**, *23*, 422; [4b] L. Hornbøll, Y. Yue, *J. Non-Cryst. Solids* **2008**, *354*, 350.
[5] [5a] R. Steendam, M. J. van Steenbergen, W. E. Hennink, H. W. Frijlink, C. F. Lerk, *J. Controlled Release* **2001**, *70*, 71; [5b] L. Yu, *Adv. Drug Deliv. Rev.* **2001**, *48*, 27; [5c] K. Kawakami, M. J. Pikal, *J. Pharm. Sci.* **2005**, *94*, 948; [5d] J. F. Mano, J. L. G. Ribelles, N. M. Alves, M. S. Sanchez, *Polymer* **2005**, *46*, 8258; [5e] Y. Wang, J. F. Mano, *J. Appl. Polym. Sci.* **2006**, *100*, 2628; [5f] J. J. Rouse, F. Mohamed, C. F. van der Walle, *Int. J. Pharm.* **2007**, *339*, 112.
[6] [6a] T. Yoshioka, N. Kawazoe, T. Tateishi, G. Chen, *Biomaterials* **2008**, *29*, 3438; [6b] T. Yoshioka, F. Kamada, N. Kawazoe, T. Tateishi, G. Chen, *Polym. Eng. Sci.* **2010**, *50*, 1895.
[7] J. Rault, *J. Phys.: Condens. Matter.* **2003**, *15*, S1193.
[8] C. Mao, S. P. Chamarthy, R. Pinal, *Pharm. Res.* **2006**, *23*, 1906.
[9] [9a] J. C. Arnold, *Polym. Eng. Sci.* **1995**, *35*, 165; [9b] A. C. M. Yang, R. C. Wang, J. H. Lin, *Polymer* **1996**, *37*, 5751; [9c] J. M. Hutchinson, S. Smith, B. Horne, G. M. Gourlay, *Macromolecules* **1999**, *32*, 5046; [9d] C. H. Ho, V. Khanh, *Theor. Appl. Fract. Mech.* **2004**, *41*, 103.
[10] A. Celli, M. Scandola, *Polymer* **1992**, *33*, 2699.
[11] P. Pan, B. Zhu, Y. Inoue, *Macromolecules* **2007**, *40*, 9664.
[12] [12a] R. J. Roe, J. J. Curro, *Macromolecules* **1983**, *16*, 428; [12b] H. H. Song, R. J. Roe, *Macromolecules* **1987**, *20*, 2723; [12c] J. Dybal, P. Schmidt, J. Baldrian, J. Kratochvil, *Macromolecules* **1998**, *31*, 6611; [12d] K. Takahara, H. Saito, T. Inoue, *Polymer* **1999**, *40*, 3729; [12e] M. Utz, A. S. Atallah, P. Robyr, A. H. Widmann, R. R. Ernst, U. W. Suter, *Macromolecules* **1999**, *32*, 6191; [12f] P. Pan, B. Zhu, T. Dong, K. Yazawa, T. Shimizu, M. Tansho, Y. Inoue, *J. Chem. Phys.* **2008**, *129*, 184902.
[13] P. Pan, Z. Liang, B. Zhu, T. Dong, Y. Inoue, *Macromolecules* **2008**, *41*, 8011.
[14] [14a] A. Gopferich, *Biomaterials* **1996**, *17*, 103; [14b] F. Burkersroda, L. Schedil, A. Gopferich, *Biomaterials* **2002**, *23*, 4221.
[15] Y. Monhammadi, E. Jabbari, *Macromol. Theory Simul.* **2006**, *15*, 643.